TENSOR-BASED ORTHOGONAL MATCHING PURSUIT WITH PHASE ROTATION FOR CHANNEL ESTIMATION IN HYBRID BEAMFORMING MIMO-OFDM SYSTEMS

Cheng-Hung Lo and Pei-Yun Tsai

Department of Electrical Engineering,
National Central University, Taiwan

ABSTRACT

Tensor decomposition is often employed for channel estimation in hybrid beamforming MIMO-OFDM systems because of multiple dimensions and channel sparsity. We propose to incorporate phase rotation in factor matrices of tensor-based orthogonal matching pursuit (T-OMP) algorithm to solve the energy leakage problem caused by the grid constraint. The phase rotation can be applied in all the dimensions of virtual channel tensor including angle of arrival (AoA), angle of departure (AoD), and delay for grid refinement. Consequently, fewer iterations are required to estimate the sparse coefficients in the core tensor. In addition, the tensor fusion technique is also proposed to further improve the performance. With the grid refinement, the number of required coefficients in the core tensor is reduced and close to the number of paths. Hence, compared to the conventional T-OMP algorithms, less computation complexity is needed while better performance can be achieved.

Index Terms—channel estimation, hybrid beamforming, MIMO-OFDM, tensor, orthogonal matching pursuit (OMP).

1. INTRODUCTION

Tensor is a multi-dimensional array that can describe objects in high-dimensional space. Tensor decomposition has been widely adopted in various fields due to the rapid growth of computation capacity and prosperous development of software package recently [1]. Rank decomposition that constructs a tensor by the sum of rank-one tensors is popular, known as canonical DECOMPosition (CANDECOMP) and the PARAllel FACtors (PARAFAC) decomposition, also called CPD. On the other hand, Tucker decomposition which expresses a tensor by its core tensor and multiple factor matrices in respective modes [2] is also an alternative. With these decomposition techniques, the essential components of a tensor can be obtained.

Tensor decomposition is gradually used in wireless communications because more dimensions are exploited to convey signals. The spatial domain is created due to antenna arrays at transmitters and receivers. Frequency domain is introduced by orthogonal frequency division multiplexing (OFDM). Hence, tensor decomposition-based hybrid beamforming in millimeter wave (mmWave) multiple-input multiple-output (MIMO)-OFDM systems has been developed [3]. Furthermore, owing to the sparsity of mmWave channel, channel estimation in hybrid-beamforming MIMO-OFDM systems through tensor decomposition attracts much attention. In [4], the wideband effect is taken into consideration. Alternating least squares (ALS) is utilized to solve the channel parameters sequentially and iteratively. The tensor-based compressive sensing (CS) approach using Tucker decomposition is employed in [5] and the authors propose joint search and sequential search for T-OMP to reduce complexity incurred by vector-based CS approaches. In [6], the authors point out that CS approaches have a limitation from the grid assumption, which causes performance error floor due to the leakage.

In this paper, a tensor-decomposition algorithm for channel estimation in hybrid beamforming MIMO-OFDM systems is presented. The aforementioned energy leakage effect not only results in degradation of sparsity but also causes contamination of estimated channel coefficients. To solve the drawback caused by the grid assumption in CS, we propose to incorporate phase rotation in the factor matrices. As a result, the number of required iterations to search for sparse representations is greatly reduced. In addition, a tensor fusion scheme is also proposed to handle the path split phenomenon. From simulation results, the proposed approach outperforms the conventional tensor-based CS with reduced complexity.

In the following, a tensor model describing the frequency-selective MIMO channels is first illustrated in Sec. 2. The proposed algorithm is presented in Sec. 3. Sec. 4 shows the simulation results and complexity comparisons. Finally, the conclusion is drawn in Sec. 5.

2. TENSOR-BASED HYBRID BEAMFORMING MIMO-OFDM SYSTEM MODEL

Fig. 1 shows the block diagram for channel estimation in hybrid beamforming MIMO-OFDM systems using N_F subcarriers with N_T transmitting antennas and N_R receiving antennas equipped in uniform linear arrays (ULAs). In addition, L_T and L_R RF chains are used at the transmitter and receiver, respectively. The channel tensor $\boldsymbol{\mathcal{G}} \in \mathbb{C}^{N_R \times N_T \times N_F}$ having L paths is constructed by outer product,

$$\boldsymbol{\mathcal{G}}(:,:,:) = \sum_{l=1}^{L} \sqrt{\frac{N_R N_T N_F}{L}} \beta_l \mathbf{a}_R(\theta_{R,l}) \circ \mathbf{a}_T(\theta_{T,l}) \circ \mathbf{a}_F(n_l) \quad (1)$$

where $\theta_{R,l}$, $\theta_{T,l}$, and β_l are AoA, AoD, and fading gain of the lth path. The normalized delay is given by $n_l = \tau_l / T_s$ with delay τ_l and sampling period T_s. For $z \in \{R, T\}$, the antenna response vector takes the form of

$$\mathbf{a}_z(\theta) = \frac{1}{\sqrt{N_z}} \left[1, e^{-j\frac{2\pi d}{\lambda}\sin(\theta)}, \dots, e^{-j\frac{2\pi(N_z-1)d}{\lambda}\sin(\theta)}\right]^T, \quad (2)$$

with $d = \lambda/2$. The frequency response vector $\mathbf{a}_F(\cdot)$ is given by

$$\mathbf{a}_F(n) = \frac{1}{\sqrt{N_F}} \left[1, e^{-j\frac{2\pi n}{N_F}}, \dots, e^{-j\frac{2\pi n(N_F-1)}{N_F}}\right]^T. \quad (3)$$

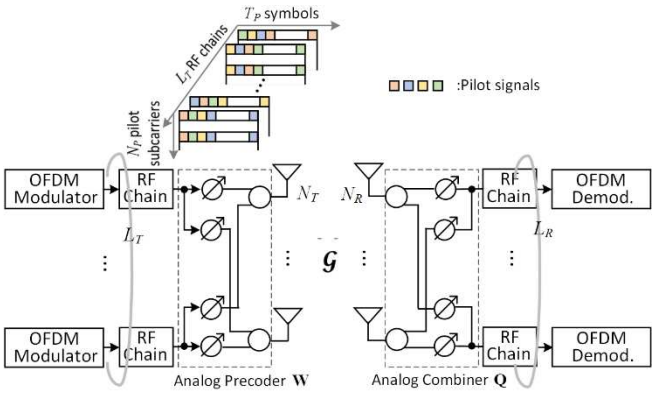

Fig. 1 Signal model of hybrid beamforming MIMO-OFDM systems.

Define selection matrix $\mathbf{S} \in \mathbb{C}^{N_P \times N_F}$ with binary elements indicating the location of N_P pilot subcarriers among N_F subcarriers. The channel frequency response $\boldsymbol{\mathcal{G}}_p$ at pilot subcarriers can be written as $\boldsymbol{\mathcal{G}}_p = \boldsymbol{\mathcal{G}} \times_3 \mathbf{S} \in \mathbb{C}^{N_R \times N_T \times N_P}$, where $\times_m$ denotes the m-mode product of a tensor and a matrix.

Assume that the same signals are transmitted at all the pilot subcarriers in one OFDM symbol. Thus, as shown in Fig. 1, the pilot signals of T_P symbols from L_T RF chains are described by the Walsh Hadamard matrix $\mathbf{D} \in \mathbb{Z}^{T_P \times L_T}$. Let $\mathbf{W} \in \mathbb{C}^{L_T \times N_T}$ be the analog precoder matrix. The signals from N_T transmitting antenna at pilot subcarriers of T_P symbols are denoted as $\mathbf{X} = \mathbf{DW} \in \mathbb{C}^{T_P \times N_T}$. At the receiver, the received signals become

$$\boldsymbol{\mathcal{Z}} = \boldsymbol{\mathcal{G}} \times_2 \mathbf{X} \times_3 \mathbf{S} + \boldsymbol{\mathcal{V}} \in \mathbb{C}^{N_R \times T_P \times N_P},$$

where $\boldsymbol{\mathcal{V}}$ represents the additive white Gaussian noise. With analog combiner $\mathbf{Q} \in \mathbb{C}^{L_R \times N_R}$, the received digital signals at pilot subcarriers are expressed as

$$\begin{aligned} \boldsymbol{\mathcal{Y}} &= \boldsymbol{\mathcal{Z}} \times_1 \mathbf{Q} \\ &= \boldsymbol{\mathcal{G}} \times_1 \mathbf{Q} \times_2 \mathbf{X} \times_3 \mathbf{S} + \boldsymbol{\mathcal{V}} \times_1 \mathbf{Q}. \in \mathbb{C}^{L_R \times T_P \times N_P}. \end{aligned} \quad (4)$$

3. CHANNEL ESTIMATION BY TENSOR-BASED ORTHOGONAL MATCHING PURSUIT WITH PHASE ROTATION

Estimation of channel tensor $\boldsymbol{\mathcal{G}} \in \mathbb{C}^{N_R \times N_T \times N_F}$ is required for designs of the precoder, combiner and signal detection. Because of path sparsity, estimation of AoA $\theta_{R,l}$ and AoD $\theta_{T,l}$ as well as path gain β_l and delay τ_l are usually performed instead of estimation of $\boldsymbol{\mathcal{G}}$ itself directly [4][5]. In [4], the ALS algorithm is used for estimation by minimizing the fitting error of respective factor matrices sequentially. The authors claim that the ALS outperforms the vector-based orthogonal matching pursuit (V-OMP) which is constrained by the grid size. In [5], the T-OMP approach is employed to take advantage of the sparsity of the core tensor and to improve the complexity of V-OMP. On the other hand, the angular rotation has been adopted in massive MIMO systems to obtain the off-grid refinement through different approaches [7][8]. In [9], the rotation is considered in OMP with the antenna switch technique. Nevertheless, the analog phase shift is not taken into consideration.

In this paper, we propose T-OMP with phase rotation for grid refinement in hybrid beamforming MIMO-OFDM systems. It has the following features.

- The T-OMP with phase rotation achieves the grid refinement in all the dimensions regarding AoA, AoD, and delay. Thus, the energy leakage problem due to the grid constraint in the conventional OMP approaches can be eliminated.
- With grid refinement, the number of required coefficients in the core tensor is decreased and close to the number of paths. Hence, few iterations implying much reduced complexity are needed.
- A tensor fusion technique is also proposed to combine estimations when the path split phenomenon takes place.

Details will be addressed in the following.

A. T-OMP with Phase Rotation

The DFT-based codebook is adopted in the phase shift of the analog precoder $\mathbf{W}$ and combiner $\mathbf{Q}$, which has the advantages of hierarchical beamforming and orthogonality. Given that $\mathbf{A}_R$, $\mathbf{A}_T$ and $\mathbf{A}_F$ are DFT matrices representing the original bases for AoA, AoD and delay and the (r, c)th element is in the form of

$$\frac{1}{\sqrt{N_Z}} e^{-j\frac{2\pi r(-N_Z/2+c)}{N_Z}} \quad (5)$$

for $Z \in \{R, T, F\}$, the channel tensor can be decomposed as

$$\boldsymbol{\mathcal{G}} = \boldsymbol{\mathcal{H}} \times_1 \mathbf{A}_R \times_2 \mathbf{A}_T \times_3 \mathbf{A}_F, \quad (6)$$

where $\boldsymbol{\mathcal{H}}$ is the core tensor associated with the virtual channel response. From (4), the received signals then can be written as

$$\boldsymbol{\mathcal{Y}} = \boldsymbol{\mathcal{H}} \times_1 \boldsymbol{\Upsilon}_R \times_2 \boldsymbol{\Upsilon}_T \times_3 \boldsymbol{\Upsilon}_F, \quad (7)$$

where $\boldsymbol{\Upsilon}_R (= \mathbf{QA}_R)$, $\boldsymbol{\Upsilon}_T (= \mathbf{XA}_T)$ and $\boldsymbol{\Upsilon}_F (= \mathbf{SA}_F)$ represent the factor matrices in three dimensions.

Define rotation matrix

$$\boldsymbol{\Gamma}_Z(\phi_Z) = diag(1, e^{-j\pi\phi_Z}, \dots, e^{-j\pi(N_Z-1)\phi_Z}). \quad (8)$$

Let channel be decomposed by rotated factor matrices, and

$$\begin{aligned} \boldsymbol{\mathcal{G}} = \boldsymbol{\mathcal{H}}^{\boldsymbol{r}} &\times_1 (\boldsymbol{\Gamma}_R(\phi_R)\mathbf{A}_R) \times_2 (\boldsymbol{\Gamma}_T(\phi_T)\mathbf{A}_T) \\ &\times_3 (\boldsymbol{\Gamma}_F(\phi_F)\mathbf{A}_F). \end{aligned} \quad (9)$$

Then, for path l, if columns c_R, c_T, and c_F of $\boldsymbol{\Gamma}_R(\phi_{R,l})\mathbf{A}_R$, $\boldsymbol{\Gamma}_T(\phi_{T.l})\mathbf{A}_T$, and $\boldsymbol{\Gamma}_F(\phi_{F,l})\mathbf{A}_F$ are equal to $\mathbf{a}_R(\theta_{R,l})$, $\mathbf{a}_T(\theta_{T,l})$, and $\mathbf{a}_F(n_l)$, then after decomposition, one grid point (c_R, c_T, c_F) in the core tensor can exactly represent the contribution of path l. In this case,

$$\begin{aligned} \phi_{R,l} &= \sin(\theta_{R,l}) - (-1 + \tfrac{2c_R}{N_R}), \\ \phi_{T,l} &= \sin(\theta_{T,l}) - (-1 + \tfrac{2c_T}{N_T}), \\ \phi_{F,l} &= \tfrac{2n_l}{N_F} - (-1 + \tfrac{2c_F}{N_F}). \end{aligned} \quad (10)$$

Given grid deviation $\epsilon = \hat{\phi}_{Z,l} - \phi_{Z,l}$, the magnitude attenuation of grid point (c_R, c_T, c_F) takes the form of

$$\Lambda(\epsilon) = \sum_{r=0}^{N_Z-1} e^{j\pi r\epsilon} = e^{j\frac{\pi}{2}(N_Z-1)\epsilon} \frac{\sin(\frac{\pi N_Z \epsilon}{2})}{N_Z \sin(\frac{\pi\epsilon}{2})} \quad (11)$$

with the estimated $\hat{\phi}_{Z,l}$. Hence, search along the direction for local maximum can help to find optimal $\phi_{Z,l}$. Fig. 2 shows the core tensors $\boldsymbol{\mathcal{H}}(:,:,c_F)$ and $\boldsymbol{\mathcal{H}}^{\boldsymbol{r}}(:,:,c_F)$ of delay c_F. It is clear that without correct rotation, the energy leakage appears owing to the off-grid AoA, AoD, and delay. However, with correct phase rotation, the grids in three dimensions are refined to proper positions and the energy is concentrated to a single point with larger magnitude. Therefore, the core tensor using rotated factor matrices becomes sparser. Fewer coefficients in $\boldsymbol{\mathcal{H}}^{\boldsymbol{r}}$ are required to reconstruct $\boldsymbol{\mathcal{G}}$ than those in $\boldsymbol{\mathcal{H}}$ and the reconstruction error floor resulted from the grid constraint can be eliminated.

Hence, the proposed T-OMP with phase rotation has the following procedure. Given the residual tensor $\boldsymbol{\mathcal{R}}^{(0)} = \boldsymbol{\mathcal{Y}}$, the sequential search starts from the dimension regarding delay. Define $\boldsymbol{\mathcal{R}}_F^{(m-1)} = \boldsymbol{\mathcal{R}}^{(m-1)}(i_1, i_2, :)$ and

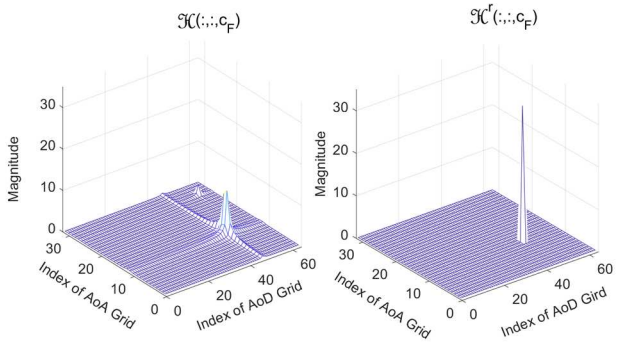

Fig. 2 Magnitude of core tensor describing virtual channel obtained by original (left) and rotated (right) factor matrices.

$$\hat{\imath}_F^{(m)} = \arg\max_{i_3} \frac{1}{L_R T_P} \sum_{i_1=1}^{L_R} \sum_{i_2=1}^{T_P} \left| \boldsymbol{\mathcal{R}}_F^{(m-1)} \times_3 \boldsymbol{\Upsilon}_F(:,i_3)^H \right|^2. \quad (12)$$

Then, an additional search using bisection method is activated to find the phase around index $\hat{\imath}_F^{(m)}$ for grid refinement.

$$\hat{\phi}_F^{(m)} = \arg\max_{\phi} \frac{1}{L_R T_P} \sum_{i_1=1}^{L_R} \sum_{i_2=1}^{T_p} \left| \boldsymbol{\mathcal{R}}_F^{(m-1)} \times_3 \boldsymbol{\Psi}_{F,\phi}\left(:,\hat{\imath}_F^{(m)}\right)^H \right|^2$$
$$\boldsymbol{\Psi}_{F,\phi}\left(:,\hat{\imath}_F^{(m)}\right) = \mathbf{S} \times \boldsymbol{\Gamma}_F(\phi) \times \mathbf{A}_F\left(:,\hat{\imath}_F^{(m)}\right). \quad (13)$$

Next, let $\boldsymbol{\mathcal{R}}_R^{(m-1)} = \boldsymbol{\mathcal{R}}^{(m-1)}(:,i_2,:) \times_3 \boldsymbol{\Psi}_{F,\hat{\phi}_F^{(m)}}\left(:,\hat{\imath}_F^{(m)}\right)^H$. The search for AoA is described by

$$\hat{\imath}_R^{(m)} = \arg\max_{i_1} \frac{1}{T_p} \sum_{i_2=1}^{T_p} \left| \boldsymbol{\mathcal{R}}_R^{(m-1)} \times_1 \bar{\boldsymbol{\Upsilon}}_R(:,i_1)^H \right|^2, \quad (14)$$

where $\bar{\mathbf{M}}$ represents column vector normalization of matrix $\mathbf{M}$ in order to generate correct correlation results when hierarchical DFT codebook is adopted. The associated phase rotation can be obtained by

$$\hat{\phi}_R^{(m)} = \arg\max_{\phi} \frac{1}{T_p} \sum_{t=1}^{T_p} \left| \boldsymbol{\mathcal{R}}_R^{(m-1)} \times_1 \bar{\boldsymbol{\Psi}}_{R,\phi}\left(:,\hat{\imath}_R^{(m)}\right)^H \right|^2$$
$$\boldsymbol{\Psi}_{R,\phi}\left(:,\hat{\imath}_R^{(m)}\right) = \mathbf{Q} \times \boldsymbol{\Gamma}_R(\phi) \times \mathbf{A}_R\left(:,\hat{\imath}_R^{(m)}\right). \quad (15)$$

Let

$$\boldsymbol{\mathcal{R}}_T^{(m-1)} = \boldsymbol{\mathcal{R}}^{(m-1)} \times_1 \bar{\boldsymbol{\Psi}}_{R,\hat{\phi}_R^{(m)}}\left(:,\hat{\imath}_R^{(m)}\right)^H \times_3 \boldsymbol{\Psi}_{F,\hat{\phi}_F^{(m)}}\left(:,\hat{\imath}_F^{(m)}\right)^H.$$

The search for AoD is given by

$$\hat{\imath}_T^{(m)} = \arg\max_{i_2} \left| \boldsymbol{\mathcal{R}}_T^{(m-1)} \times_2 \bar{\boldsymbol{\Upsilon}}_T(:,i_2)^H \right|^2, \quad (16)$$

and the phase for grid refinement is calculated by

$$\hat{\phi}_T^{(m)} = \arg\max_{\phi} \left| \boldsymbol{\mathcal{R}}_T^{(m-1)} \times_2 \bar{\boldsymbol{\Psi}}_{T,\phi}\left(:,\hat{\imath}_T^{(m)}\right)^H \right|^2$$
$$\boldsymbol{\Psi}_{T,\phi}\left(:,\hat{\imath}_T^{(m)}\right) = \mathbf{X} \times \boldsymbol{\Gamma}_T(\phi) \times \mathbf{A}_T\left(:,\hat{\imath}_T^{(m)}\right). \quad (17)$$

The selected basis with grid refinement is augmented in respective dimensions as

$$\boldsymbol{\Psi}_Z^{(m)} = \left[\boldsymbol{\Psi}_Z^{(m-1)} \quad \boldsymbol{\Psi}_{Z,\hat{\phi}_Z^{(m)}}\left(:,\hat{\imath}_Z^{(m)}\right)\right]. \quad (18)$$

Thereafter, the coefficients in the core tensor are estimated by pseudo inverse

$$\mathbf{B}^{(m)} = \left(\boldsymbol{\Psi}_F^{(m)} \odot \boldsymbol{\Psi}_T^{(m)} \odot \boldsymbol{\Psi}_R^{(m)}\right)^{\dagger} \mathrm{vec}(\boldsymbol{\mathcal{Y}}), \quad (19)$$

where $\odot$ denotes the Khatri-Rao product and $\mathrm{vec}(\cdot)$ vectorizes the tensor $\boldsymbol{\mathcal{Y}}$. The residual tensor is computed by

$$\boldsymbol{\mathcal{R}}^{(m)} = \boldsymbol{\mathcal{R}}^{(0)} - \sum_{s=1}^{m} \mathbf{B}^{(m)}(s) \cdot \boldsymbol{\Psi}_R^{(m)}(:,s) \circ \boldsymbol{\Psi}_T^{(m)}(:,s) \circ \boldsymbol{\Psi}_F^{(m)}(:,s). \quad (20)$$

Algorithm 1 T-OMP with Phase Rotation and Tensor Fusion
Input: received signal $\boldsymbol{\mathcal{Y}}$ and original factor matrices $\boldsymbol{\Upsilon}_R, \boldsymbol{\Upsilon}_T, \boldsymbol{\Upsilon}_F$
Output: reconstructed channel tensor $\widehat{\boldsymbol{\mathcal{G}}}$
Initialization: $\boldsymbol{\Psi}_Z^{(0)} = [\,]$ for $Z \in \{R,T,F\}$, $\boldsymbol{\mathcal{R}}^{(0)} = \boldsymbol{\mathcal{Y}}$, $m = 1$,
1. Solve (12) and (13) to obtain $\hat{\imath}_F^{(m)}$ and $\hat{\phi}_F^{(m)}$.
2. Solve (14) and (15) to obtain $\hat{\imath}_R^{(m)}$ and $\hat{\phi}_R^{(m)}$.
3. Solve (16) and (17) to obtain $\hat{\imath}_T^{(m)}$ and $\hat{\phi}_T^{(m)}$
4. Basis augmentation by (18)
5. Estimation of core tensor coefficients by (19)
6. Computation of residual tensor by (20)
7. $m = m + 1$. Repeat from Step 1 until $m = M + 1$
8. If tensor fusion is necessary, $k = 1$, else go to Step 13
9. Update factor matrices and coefficients by (22) and (23)
10. Update residual tensor and basis by (24) and (25)
11. Estimation of core tensor coefficients by (19)
12. $k = k + 1$. Repeat from Step 10 until $k = K + 1$
13. Reconstruct channel tensor by (26)

B. Tensor Fusion

In some case, because of the noise and interference in the virtual channel space, the components of one path with strong gain are split into two estimations having similar AoAs and AoDs but quite imbalanced gains. Tensor fusion then starts to combine two estimations into one.

Assume that M iterations are performed by T-OMP with phase rotation. The final selected basis in the delay direction is first examined. The estimation of delay $\hat{n}_m$ can be restored by index $\hat{\imath}_F^{(m)}$ and phase $\hat{\phi}_F^{(m)}$. From (3) and (10),

$$\hat{n}_m = \left(-\frac{N_F}{2} + \hat{\imath}_F^{(m)}\right) + \frac{N_F}{2}\hat{\phi}_F^{(m)}. \quad (21)$$

Usually, cyclic prefix consists of signal samples less than or equal to $N_F/4$, the search range of $\hat{\imath}_F^{(m)}$ in (12) is limited to keep $\hat{n}_m$ in the range of $\left[0, \frac{N_F}{4}\right]$. Assume that there exist K sets of close estimations that satisfy $\left|\hat{n}_{q_k} - \hat{n}_{p_k}\right| < \delta$ for index $q_k > p_k$ and $k = 1, \ldots, K$, where δ denotes the threshold. In this case, the q_kth selected basis can be fused into the p_kth selected basis.

First, the undesired vectors are removed by

$$\boldsymbol{\Psi}_Z^{(M)} = \boldsymbol{\Psi}_Z^{(M)} \setminus \left[\boldsymbol{\Psi}_{Z,\hat{\phi}_Z^{(p_k)}}\left(:,\hat{\imath}_Z^{(p_k)}\right) \quad \boldsymbol{\Psi}_{Z,\hat{\phi}_Z^{(q_k)}}\left(:,\hat{\imath}_Z^{(q_k)}\right)\right] \quad (22)$$

and their associated coefficients are also nullified by

$$\mathbf{B}^{(M)}(p_k) = \mathbf{B}^{(M)}(q_k) = [\,]. \quad (23)$$

For tensor fusion, the residual tensor is recalculated as

$$\boldsymbol{\mathcal{R}}^{(M+k-1)} = \boldsymbol{\mathcal{R}}^{(0)} - \sum_{s=1}^{M-2K+k-1} \mathbf{B}^{(M+k-1)}(s) \cdot \boldsymbol{\Psi}_R^{(M+k-1)}(:,s) \circ \boldsymbol{\Psi}_T^{(M+k-1)}(:,s) \circ \boldsymbol{\Psi}_F^{(M+k-1)}(:,s). \quad (24)$$

Repeat (14) to (17) for $m = M + k$ and $\hat{\imath}_F^{(M+k)} = \hat{\imath}_F^{(p_k)}$, $\hat{\phi}_F^{(M+k)} = \hat{\phi}_F^{(p_k)}$ to estimate $\hat{\imath}_R^{(M+k)}$, $\hat{\phi}_R^{(M+k)}$, $\hat{\imath}_T^{(M+k)}$, and $\hat{\phi}_T^{(M+k)}$ again. The selected basis is updated with the new one.

$$\boldsymbol{\Psi}_Z^{(M+k)} = \left[\boldsymbol{\Psi}_Z^{(M+k-1)} \quad \boldsymbol{\Psi}_{Z,\hat{\phi}_Z^{(M+k)}}\left(:,\hat{\imath}_Z^{(M+k)}\right)\right], \quad (25)$$

for $k = 1, \ldots, K$. Accordingly, the coefficients are estimated by (19) with the updated basis again. The channel tensor is then reconstructed by

$$\widehat{\boldsymbol{\mathcal{G}}} = \sum_{s=1, s\neq p_k, q_k}^{M+K} \mathbf{H}^r\left(\hat{\imath}_R^{(s)}, \hat{\imath}_T^{(s)}, \hat{\imath}_F^{(s)}\right) \left(\boldsymbol{\Gamma}_R\left(\hat{\phi}_R^{(s)}\right)\mathbf{A}_R\left(:,\hat{\imath}_R^{(s)}\right)\right) \circ \left(\boldsymbol{\Gamma}_T\left(\hat{\phi}_T^{(s)}\right)\mathbf{A}_T\left(:,\hat{\imath}_T^{(s)}\right)\right) \circ \left(\boldsymbol{\Gamma}_F\left(\hat{\phi}_F^{(s)}\right)\mathbf{A}_F\left(:,\hat{\imath}_F^{(s)}\right)\right), \quad (26)$$

where $\mathbf{H}^{r}\left(\hat{\imath}_R^{(s)}, \hat{\imath}_T^{(s)}, \hat{\imath}_F^{(s)}\right)$ indicates coefficients from $\mathbf{B}^{(M+K)}$ in (19) mapped by $\hat{\imath}_R^{(s)}$, $\hat{\imath}_T^{(s)}$, and $\hat{\imath}_F^{(s)}$. The pseudo codes of the whole procedure are provided in Algorithm 1.

4. SIMULATION RESULTS

The performance of the proposed algorithm is then simulated and verified. The hybrid beamforming MIMO-OFDM system uses ULA with $N_T = 64$, $N_R = 32$, and FFT size $N_F = 1024$. Assume that $L_T = L_R = 8$ at both the transmitter and the receiver. In order to reduce sensing time, 16-point low-level DFT codebook with zero padding is adopted for $\mathbf{Q}$ and $\mathbf{W}$ while 32-point, 64-point, and 1024-point DFT matrices are used for $\mathbf{A}_R$, $\mathbf{A}_T$, and $\mathbf{A}_F$. Four sets of codewords are transmitted. In the training phase, T_P =8 training symbols and $N_P = 256$ pilot subcarriers are observed. The 6-path ($L = 6$) Rayleigh fading channels are randomly generated with AoA and AoD uniformly distributed from $-\pi/2$ to $\pi/2$. The channel delay follows the exponential distribution with mean 14ns and has a resolvable spacing of at least 1ns from the analog-to digital converter (ADC) resolution. Hence, $\delta = 1$ for tensor fusion. The estimation performance is evaluated by NMSE, which is given by

$$\text{NMSE} = E\left\{\frac{\|\mathcal{G}-\hat{\mathcal{G}}\|_2^2}{\|\mathcal{G}\|_2^2}\right\}. \tag{27}$$

Fig. 3 shows the performance of the proposed T-OMP with phase rotation (T-OMP-R) that uses different resolutions in the virtual channel domain when we search $\hat{\phi}_F^{(m)}$, $\hat{\phi}_R^{(m)}$, $\hat{\phi}_T^{(m)}$ by the bisection method. The number of iterations M is set to 8. Obviously, the higher the resolution for grid refinement, the better the performance is. The improvement of tensor fusion is also clear. Fig. 4 provides the performance comparison with other algorithms. The T-OMP sequential search (T-OMP-SS) uses random phase shift in the analog precoder and combiner [5]. Random probing in the spatial domain with arbitrary gain occurs and sometimes the selected basis can only generate effective channel $\widehat{\mathcal{G}}_{eff}$ that is similar to $\mathcal{G}_{eff} = \mathcal{G} \times_1 \mathbf{Q} \times_2 \mathbf{W}$. The CPD method utilizes the ALS algorithm [4]. The resolution in the search process to derive AoA, AoD, and delay is also set as indicated. Note that resolutions of T-OMP-R and CPD method are defined in the virtual channel domain and in the spatial angle domain, respectively. The proposed T-OMP-R has better NMSE in low to middle SNR regions. The achievable spectral efficiency can be enhanced from improved channel estimation error [10].

The complexity of the algorithms mentioned above is then assessed. The CPD method [4] needs to solve three least squares (LS) equations. Assume that $\min(L_R, N_P, T_P) > L$, the complexity of complex multiplications (Mul.) in an LS equation can be described by $\mathcal{O}(L_R N_P T_P L)$. The matrix dimension for inversion (Inv.) is comparable to the number of paths. In the simulation, more than 100 iterations are used. Although extra searches of proper phase rotation are required in T-OMP-R, the bisection method greatly reduces search efforts for the refinement. Given that V_F, V_R, and V_T denote the sizes of respective search spaces, the matrix multiplications of T-OMP-R can be described by $L_R N_P T_P (V_F + C)$ in the delay dimension, where $C = 10$ if the resolution is 2^{-10}. Compared to $V_F (= 256)$, the overhead of C is not large. Thanks to the grid refinement, the number of sparse coefficients in core tensor is comparable to the number of paths, which significantly reduces the required iterations. T-OMP-SS needs to gather more than five times the

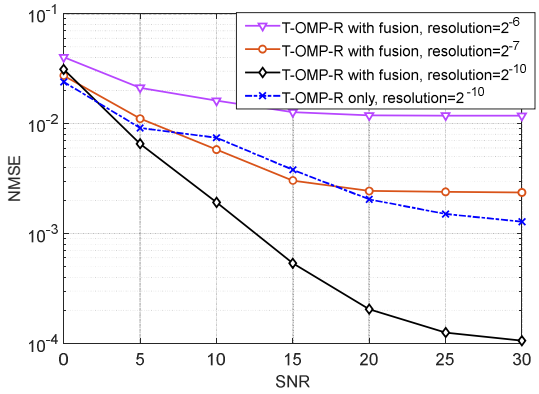

Fig. 3 Performance of T-OMP-R with and without tensor fusion under different settings of resolution.

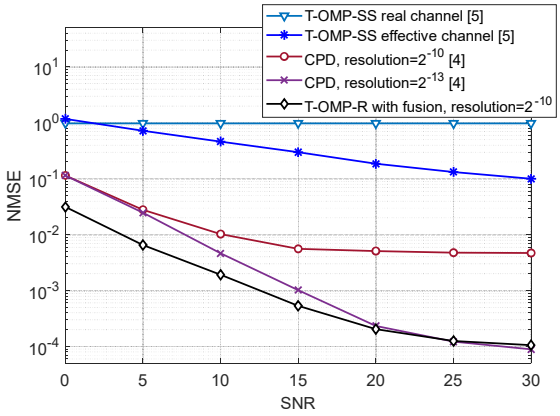

Fig. 4 Performance comparison of different algorithms.

Table I Complexity Comparison

	Matrix Mul.	Matrix Inv.	Iterations
CPD [4]	$\mathcal{O}(3L_R N_P T_P L)$	$\mathcal{O}(3L^3)$	> 100
T-OMP-SS [5]	$\mathcal{O}(L_R N_P T_P V_F + L_R T_P V_R + T_P V_T)$	$\mathcal{O}((5L)^3)$	$\sim 5L$
T-OMP-R	$\mathcal{O}(L_R N_P T_P (V_F + C) + L_R T_P (V_R + C) + T_P (V_T + C))$	$\mathcal{O}(L^3)$	$\sim L$

coefficients in the core tensor but still suffers energy leakage. Table I summarizes the complexity in the dimensions of delay, AoA, and AoD. Although $V_F (= 256) > 3L$, the CPD method needs several hundreds of iterations to ensure convergence, the reduced iterations of T-OMP-R still bring advantages.

5. CONCLUSION

Channel estimation in mmWave hybrid beamforming MIMO-OFDM systems can be described by a tensor model. The proposed T-OMP with phase rotation can achieve grid refinement to solve the energy leakage problem and the performance error floor is eliminated. In addition, phase rotation can be applied to the factor matrices in all the dimensions so that the number of iterations to acquire the required coefficients in the core tensor can be significantly reduced. The proposed tensor fusion technique can further improve the performance. Because of fewer iterations, the less computation complexity is consumed as opposed to the conventional T-OMP algorithms.

REFERENCES

[1] T. G. Kolda and B. W. Bader, "Tensor decompositions and applications, " *SIAM Rev.*, vol. 51, no. 3, pp. 455-500, 2009.

[2] N. D. Sidiropoulos, L. De Lathauwer, X. Fu, K. Huang, E. E. Papalexakis and C. Faloutsos, "Tensor Decomposition for Signal Processing and Machine Learning," *IEEE Transactions on Signal Processing*, vol. 65, no. 13, pp. 3551-3582, 1 July1, 2017

[3] G. M. Zilli, W. P. Zhu, "Constrained tensor decomposition based mmWave Massive MIMIO-OFDM communication systems," *IEEE Transactions on Vehicular Technology*, vol. 6, Iss. 6, pp. 5775-5788, Jun. 2021.

[4] Z. Zhou, J. Fang, L. Yang, H. Li, Z. Chen and R. S. Blum, "Low-Rank Tensor Decomposition-Aided Channel Estimation for Millimeter Wave MIMO-OFDM Systems," *IEEE Journal on Selected Areas in Communications*, vol. 35, no. 7, pp. 1524-1538, July 2017.

[5] D. C. Araújo, A. L. F. de Almeida, J. P. C. L. Da Costa and R. T. de Sousa, "Tensor-Based Channel Estimation for Massive MIMO-OFDM Systems," *IEEE Access*, vol. 7, pp. 42133-42147, 2019.

[6] J. Zhang, D. Rakhimov, and M. Haardt, "Gridless channel estimation for hybrid mmWave MIMO systems via tensor-ESPRIT algorithms in DFT beamspace," *IEEE Journal of Selected Topics in Signal Processing*, vol. 15, no. 3, pp. 816-831, Apr. 2021.

[7] J. Dai, A. Liu, and V. K. N. Lau, "FDD massive MIMO channel estimation with arbitrary 2D-array geometry," *IEEE Transactions on Signal Processing*, vol. 66, pp. 2584-2599, May 2018.

[8] D. Fan, F. Gao, G. Wang, Z. Zhong, and A. Nallanathan, "Angle Domain Signal Processing-Aided Channel Estimation for Indoor 60-GHz TDD/FDD Massive MIMO Systems" *IEEE Journal on Selected Areas in Communications*, vol. 35, pp. 1948-1961, Sep. 2017.

[9] J. Huang, H. Wei, P. Li, J. Li and D. Wang, "Decomposition estimation for mmWave channel based on OMP with rotation operation," *International Conference on Wireless Communications and Signal Processing (WCSP)*, 2019, pp. 1-5.

[10] J. Lee, G. -T. Gil and Y. H. Lee, "Channel Estimation via Orthogonal Matching Pursuit for Hybrid MIMO Systems in Millimeter Wave Communications," *IEEE Transactions on Communications*, vol. 64, no. 6, pp. 2370-2386, June 2016.